Colloids and Surfaces A: Physicochemical and Engineering Aspects 676 (2023) 132289

Contents lists available at ScienceDirect

Colloids and Surfaces A: Physicochemical and Engineering Aspects

journal homepage: www.elsevier.com/locate/colsurfa

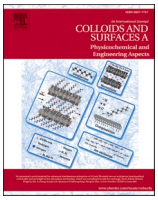

Effects of ultrasound on the removal of emulsion plugging in oil reservoirs

Ephraim Otumudia, Hossein Hamidi *, Prashant Jadhawar, Kejian Wu

School of Engineering, King's College, University of Aberdeen, Aberdeen AB24 3UE, United Kingdom

GRAPHICAL ABSTRACT

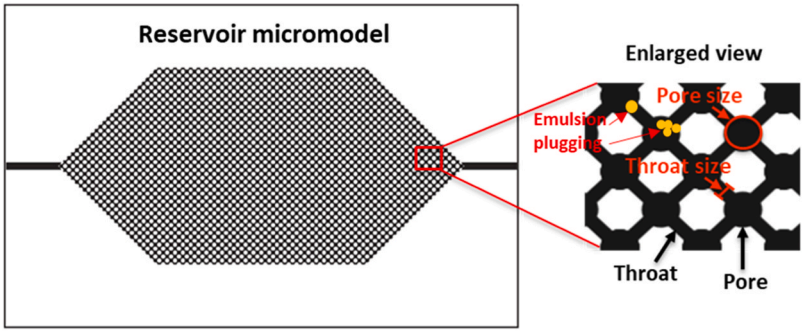

ARTICLE INFO

Keywords:
Ultrasound
Formation damage
Emulsion plugging
Glass micromodel
Image analysis

ABSTRACT

The generation of water-in-crude oil emulsions in a reservoir can cause formation damage due to droplet trapping at pore spaces. The removal of the damage is anticipated to be inexpensive and eco-friendly when done with ultrasound as opposed to chemical demulsifiers. The influence of ultrasonic power and frequencies on the removal process, however, is not well understood. Additionally, the process's underlying mechanism is largely speculated. In this study, the effect of ultrasound on the removal of emulsion plugging in oil reservoirs was investigated using a glass micromodel. Emulsion blockage during oil production was replicated in the micromodel and subjected to different ultrasonic frequencies (20 and 40 kHz) and powers (100–1000 watt). The experiments demonstrate that when ultrasonic power and frequency increase from 100 to 1000 watt and 20–40 kHz, respectively, demulsification effectiveness decreases. Ultrasound at low frequency (20 kHz) and power (100 watt) proved to be the most efficient condition to dislodge trapped emulsions in the micromodel pores, facilitate droplet coalescence and increase fluid recovery. The percentage of recovered emulsions increased to 58 % when the micromodel was exposed to ultrasound (20 kHz, 100 watt), as opposed to 53.3 % in the case without ultrasound. This study provides insights into the microscopic behavior of emulsions under the influence of ultrasonic waves, allowing petroleum engineers to optimize ultrasound demulsification process.

1. Introduction

Reservoir engineers frequently use secondary recovery techniques such as waterflooding to aid production. However, in an offshore setting with limited water supplies, seawater or formation brine is often employed as the source of flooding. When this brine is introduced into

* Corresponding author.
E-mail address: hossein.hamidi@abdn.ac.uk (H. Hamidi).

https://doi.org/10.1016/j.colsurfa.2023.132289
Received 14 April 2023; Received in revised form 21 August 2023; Accepted 22 August 2023
Available online 23 August 2023

the reservoir, it can induce water-in-oil (w/o) emulsions at any location in the reservoir. The development of stable water-in-crude oil emulsions can significantly impede fluid flow in the reservoir or near the wellbore, due to entrapment of emulsion droplets in pore spaces, increased fluid viscosity and lower effective permeability. This has the consequence of lowering production and decreasing profits. There are many ways to treat emulsions problems, including introducing coagulants, using microbial metabolism, and flotation techniques [1]. A common way of treating emulsion problems in oil reservoirs is by the injection of chemical demulsifiers. The chemicals breakdown emulsions by adsorbing onto the oil-water interface and reducing its interfacial tension [2]. This remedial method is expensive and could lead to environmental pollution [3,4]. While experimental investigations on this subject are lacking, a few researches suggest that ultrasound, as a low-cost and pollution-free technology, may be used as a substitute to remediate emulsion challenges in oil reservoirs. Xie et al. [5] investigated the use of acoustics for water droplet coalescence and crude oil emulsion dehydration. Their study focused on the effects of ultrasonic irradiation on crude oil emulsion parameters such as viscosity, water drop radius, and shear strength of the oil-water interfacial film. These characteristics are critical for the coalescence of water drops in a water-oil emulsion during the ultrasonic oil separation process. They discovered that ultrasonic treatment weakens the interfacial film in crude emulsions and decreases emulsion stability.

Luo et al. [6] used 20.9 kHz ultrasonic standing waves to separate water from mineral oil and discovered that when oil viscosity increases, a greater optimum acoustic intensity is required. The droplet size and starting water content have an impact on separation efficiency.

The viability of employing a 35 kHz ultrasound to demulsify crude emulsions was examined and coalescing of water droplets (especially smaller droplets) was observed for all emulsions tested [7]. Demulsification efficiency of up to 65 % was achieved for emulsions containing 50 % water [7]. However, it was also found that demulsification efficiency for a 20 kHz ultrasound drops quickly when the initial water content of the emulsion exceeds 20–50 % [8,9].

Atehortúa et al. [10] utilized high-frequency ultrasonic standing waves to examine the separation of water in crude oil emulsions by ultrasound. It was found that ultrasound energy promotes the coalescing of water droplets at the pressure nodes of the wave field. In addition, five experiments conducted demonstrated that ultrasonic standing wave reduces the quantity of water in the emulsions.

Nii et al. [11] separated oil-in-water emulsions using ultrasonic standing waves at a frequency of 2 MHz. Oil droplets were transported to the antinodal planes, where they coalesced into larger droplets. At the end of the sonication, the larger droplets rise at a quicker pace which is attributed to the increase in buoyancy forces with increasing droplet size. However, Garcia-Lopez and Sinha [12] discovered challenges in using ultrasound energy to separate industrial oil-in-water emulsions. The following hurdles exist: (a) emulsion stability due to surfactants, (b) oil concentration, and (c) oil droplet size. The coalescence of droplets on the wave's antinodal planes determines the success of ultrasound emulsion breakdown. When cavitation bubbles are exposed to ultrasound, they move to pressure antinodes and coalesce [13].

Ultrasound might also be used as a supplement to minimize the amount of chemical demulsifiers used in the coalescence process and the removal of water droplets in emulsions. Check et al. [14] combined ultrasound and demulsifiers to remove water from crude emulsions. The impact of ultrasound power and sonication time on the removal efficiencies of water were examined, and the obtained findings showed that determining the optimum parameters is critical to avoiding substantial reduction in the water removal efficiencies. The application of an optimal ultrasound power of 57.7 W, sonication time of 6.2 min at 100 °C, 2 ppm chemical demulsifiers and 60 min settling time resulted in water removal efficiency of about 99.8 %.

Most previous studies on ultrasonic technology for emulsion breakdown have been on microscale applications in the fields of biological materials and petrochemical industries. In the oil industry, there is limited research on the use of ultrasound to treat water-in-oil emulsions problems in oil reservoirs, and there are no laboratory studies that evaluated the mechanism of ultrasound in combating emulsion problems in oil reservoirs. In this study, the influence of ultrasonic waves on the removal of emulsion plugging during oil production was investigated, using a two-dimensional glass micromodel as a representation of an oil reservoir. Emulsion plugging during oil production was reproduced in the micromodel, which was subsequently subjected to ultrasonic waves of various frequencies (20 and 40 kHz) and powers (100 – 1000 watts). Glass is similar to sandstone rock in that both are largely made up of silicon dioxide. While real sandstone formations have intricate pore geometries, variations in pore sizes, and complex connectivity that affect fluid flow, which cannot be accurately represented in a two-D micromodel, the micromodel is a simplification of the complex structure of a real formation, which has been utilized in recent studies by researchers [15–21] for emulsion entrapment studies [16]. To the best of our knowledge, this is the first microscopic visualization report of ultrasound demulsification utilizing this small-scale reservoir rock model. This opens a unique window into the microscopic behavior of emulsions within oil reservoirs and providing insights that contribute to demulsification by the influence of ultrasonic waves. With good understanding of these mechanisms, petroleum engineers will better predict emulsion behaviors and optimize ultrasound demulsification processes.

2. Experimental set-up and procedure

2.1. Materials

To establish initial water saturation in the micromodel, brine was utilized as the formation water. The brine were synthesized to achieve the objective of emulsion plugging by dissolving NaCl, Na_2SO_4, $MgCl_2$, $CaCl_2$ and KCl (provided by Sigma Aldrich UK) uniformly in deionized water. Table 1 shows the concentration of the salt components for the various brines used in this study [22].

North-sea crude oil (used as the oil phase) was diluted with toluene in a ratio of 50:50 to reduce viscosity and ease the flow of the crude in the micromodel. Toluene, acetone and distilled water were used as cleaning agents. The fluid properties are shown in Table 2. The fluid densities were measured with Anton Paar™ Viscometer.

2.2. Experimental set-up and equipment

Two-D glass micromodel used in this study were constructed with high-contrast patterns to depict the pore network of an oil reservoir. The pore geometry is represented by the circular pore body form shown in Fig. 1.

Table 3 lists the physical and hydraulic characteristics of the micromodel. Image analysis was used to estimate the micromodel's porosity. After saturating the micromodel with colored distilled water, it was photographed using a high-resolution digital camera. The ratio of the colored area of the micromodel to the overall area of the micromodel is known as porosity.

A water bath manufactured with acrylic material (L: 63 cm, W: 43 cm, H: 30 cm) was filled with water, and a stainless-steel, water-

Table 1
Brine composition [22].

Component	Salt Concentration (g/100 ml)
NaCl	2.8
Na_2SO_4	0.5
$MgCl_2$	0.2
$CaCl_2$	0.1
kCl	0.1

Table 2
Fluid properties.

Fluid Properties	Fluid		
	Crude	Toluene	Acetone
Density at 15 °C (g/cm3)	0.887	0.869	0.808
Molecular weight (g/mol)	318	92.14	58.08

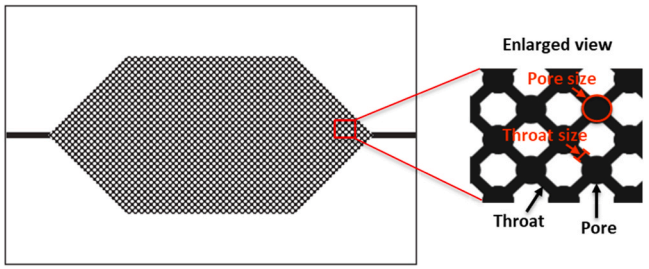

Fig. 1. Uniformly sized micromodel, with circular pore shape.

proofed immersible transducer (L: 53 cm, W: 33 cm, H: 9 cm) was attached to the bath's bottom and connected to digital ultrasonic generators (purchased from Beijing Ultrasonic). The water in the bath creates an environment for the ultrasonic waves to propagate. Two digital ultrasonic generators (purchased from Beijing Ultrasonic), each with an adjustable power range of 100–1000 watts and fixed frequencies of 20 and 40 kHz, were used. A bespoke micromodel holder holds the micromodel 5 cm above the surface of the transducer. The micromodel was immersed in the water, leaving the top surface water-free for high-quality photographs. The temperature rise induced by ultrasound was measured using a temperature probe placed within the acrylic water tank. To introduce and control fluid flow in the micromodel system, a syringe pump (PHD Ultra, Harvard Apparatus) was utilized. A temperature probe was inserted within the acrylic water tank to monitor the increase in temperature caused by ultrasound. Olympus BX60M microscope was used to aid emulsion screening while TA HR-3 Rheometer was used to assess the rheological behavior of emulsions. In the micromodel, the effect of ultrasound on the behavior of the emulsions was recorded and captured using Dino-lite (AM7915MZT) digital microscope, with a light source and computer connection. A vortex mixer was used to formulate emulsion while Anton PaarTM viscometer was used to measure fluid properties. Fig. 2 depicts a schematic of the experimental setup.

2.3. Experimental procedure

2.3.1. Formulation of emulsion and droplet size analysis

The w/o emulsions used in this study was prepared by putting crude oil in a test tube and using a vortex mixer to mix the crude oil with synthetic brine at 1000 rpm. The brine is gently added to the crude and thoroughly mixed for 15 min.

Table 4 shows the properties of the water-oil (w/o) emulsions at 20 °C. The densities and kinematic viscosities were measured using an Anton Paar™ Viscometer.

The droplet size distribution is an effective method for determining the stability of emulsions [23]. Thus, the emulsions' stability was examined using microscopic photography and droplet size distribution analysis. Emulsion samples are collected from the test tube (H: 15 cm, D: 1.5 cm) and transferred to a microscope slide to be photographed under an Olympus BX60M microscope with a magnification of 100x. The sample photographs are taken from bottom, middle and top areas along the height of the test tube at 0, 5, 20, 40,50 and 120 min after emulsion preparation under static conditions. Several pictures were taken for each sample, and the water droplets were processed, detected, counted, and measured using ImageJ processing software. ImageJ converts the pixel values of each droplet to an area (μm^2) unit and the results were exported to Excel software to be converted to droplet diameter and presented as droplet size distribution plots. For each sample period, at least 10 images with a minimum of 500 droplets from each emulsion solution were analyzed [22]. Fig. 3 illustrates how ImageJ was used to analyze an example image.

The captured picture (Fig. 3a) was converted to grayscale (Fig. 3b), and the ImageJ processing tool detects the water droplets (white circles in Fig. 3c), which were then counted and measured (Fig. 3d). During the analysis, the thresholding is manually adjusted to ensure all real droplets were detected and counted, as shown in Fig. 3(c and d).

2.3.2. Procedure for micromodel experiments and analysis

Before conducting experiments, the micromodel was cleaned with toluene, acetone, and distilled water, followed by vacuuming and 12 h of 100 °C oven drying. All the components of the experiment were cleaned and dried to ensure that they are dirt-free. To recreate the scenario of emulsion plugging in the micromodels, the following were undertaken. First, several pore volumes (PV) of brine were injected into the micromodel until it was fully saturated, and the flow becomes steady, after which the system was left undisturbed for 3 h to equilibrate. Following this, the water-in-oil emulsion was introduced into the micromodel to displace brine until brine production ceases and connate water saturation is achieved. Injecting crude emulsions (dark brown) into the micromodel may cause pore space blockages due to the nature of the selected emulsions.

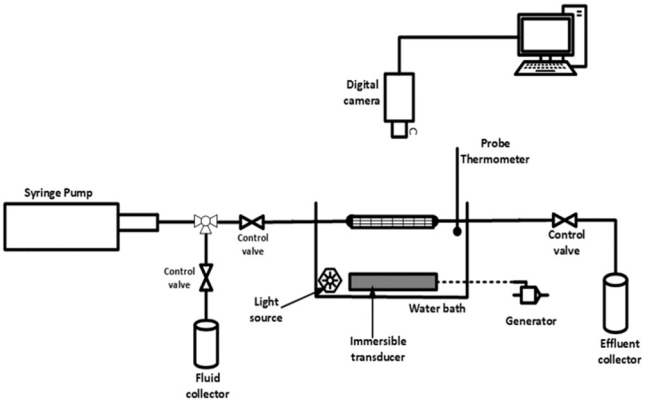

Fig. 2. Schematic of experiment setup.

Table 4
Properties of water-oil (w/o) emulsion.

Fluid properties @ 20 °C		Water/oil ratio	Sampling Time (min)
Density (g/cm^3)	Kinematic viscosity (mm^2/s)		
1.0212	1.1096	3:10	0–120

Table 3
Design properties of Two-D glass micromodel.

Glass dimension (L*W), mm	Pattern dimension (L*W), mm	Etched depth, μm	Co-ordination number	Pore size, μm	Throat size, μm	Aspect Ratio	Porosity
110 * 69	87.5 * 42.3	100	4	800	300	2.67	0.46

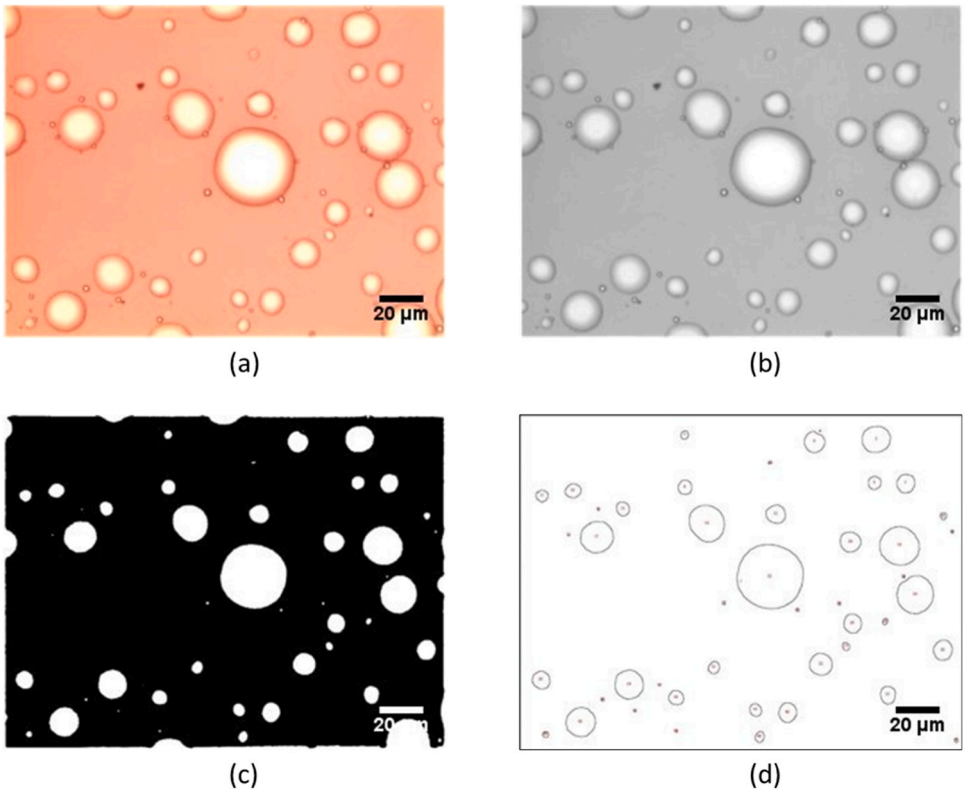

Fig. 3. Procedure for emulsion screening (a) original image, (b) converted to grayscale, (c) droplet detection (d) droplet counting and analysis.

Waterflooding operations (with the same brine used for emulsion preparation), were then carried out in the micromodel without ultrasound until the emulsion is no longer produced and residual emulsion saturation is reached. During the waterflooding, pink dye was added to the brine to allow distinction of phases in the micromodel and the plugging effect of w/o emulsion on emulsion recovery (the emulsion mixture is primarily oil) is observed throughout the operation. To investigate the effect of ultrasound on emulsion plugging during recovery of emulsions, the abovementioned procedure was repeated under the same conditions, with waterflooding done under the influence of ultrasound. The micromodel was sonicated at different ultrasonic frequencies and powers to see how the ultrasound parameter affects the results. All fluids were injected at a constant rate of 0.6 ml/hr to guarantee laminar flow in the micromodel. To ensure repeatability, the micromodel experiments were conducted three times, and the average values with standard deviation errors were presented. Repeated experiments showed an average error of not more than 5 % and the general trend remained the same. All experiments were conducted under ambient conditions.

Continuous video recording and high-quality images of the micromodel acquired during the experiment were required for obtaining qualitative and quantitative data analysis on the effects of ultrasonic waves on emulsion plugging removal. A high-resolution digital microscope (Dino-lite Edge AM7915MZT) was used to record and capture the images. Pore scale images were captured at 230x magnification. The image of the whole micromodel is segmented into three phases using ImageJ's Trainable Weka Segmentation plugin to offer strong color differentiation of the emulsions, brine, and glass phases in the micromodel, as seen in Fig. 4. In the raw image, the emulsions, brine, and glass phases are dark-brown, pink, and light gray, respectively, but in the segmented image, the phases are emulsions (red), brine (green), and glass (purple). Finally, the segmented image was imported into MATLAB, where the number of pixels in each phase was counted and the fluid saturation before and after ultrasonic treatment was estimated.

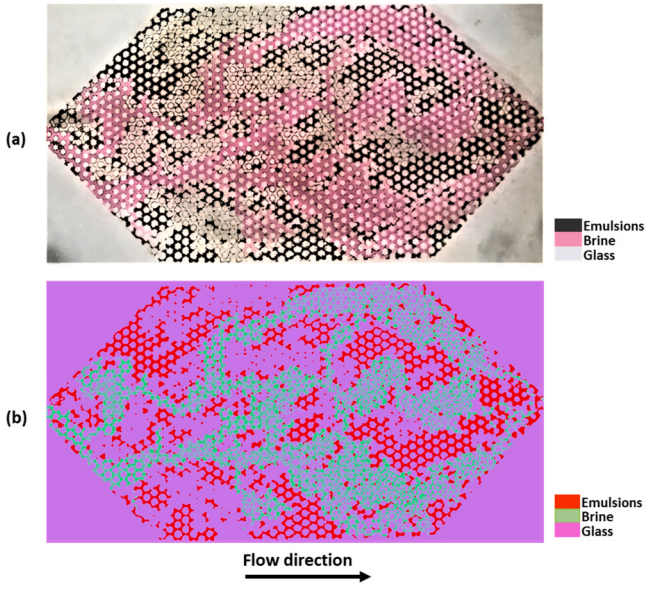

Fig. 4. Sample image showing segmentation of phases using trainable Weka segmentation, (a) raw image captured by camera, (b) segmented image.

The following relationship is used to compute the percentage of recovered emulsions during sonication:

$$E_R(\%) = \frac{E_{t0} - E_{tn}}{E_{t0}} \times 100$$

Where E_R denotes the recovered emulsions, E_{t0} and E_{tn} denotes the area of micromodel's pore spaces occupied by emulsions at sonication times 0 and n respectively.

3. Results and discussion

3.1. Analysis of emulsion stability

The stability of the emulsion was analyzed to affirm the suitability of the emulsion system for the micromodel experiment. The ideal emulsion would be a slightly stable emulsion with some droplet sizes larger than the micromodel's pore and throat diameters and these are predicted to block the micromodel's flow networks during fluid movement owing to strain and emulsion entrapment. The ability for droplet aggregation which can result in pore blockage in the micromodel system also makes an ideal emulsion for the micromodel experiments. It is also worth noting that the creation of stable and large water-in-oil emulsion droplets can significantly restrict fluid flow in the reservoir due to an increase in fluid viscosity [24,25].

Figs. 5 and 6 show microscopic views of the emulsion sample 0, 5, 20, 40, 60, and 120 min after preparation, and their droplet size distributions respectively. The white and orange regions are water droplets and the oil phase, respectively.

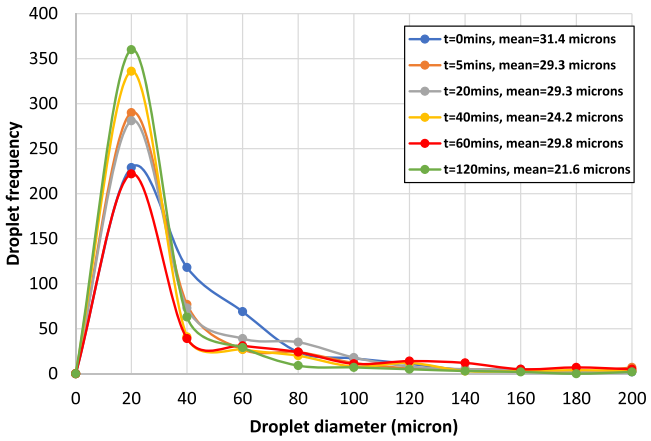

Fig. 6. Emulsion droplet size distribution taken from several images, 0, 5, 20, 40, 60, 120 min after preparation of emulsion.

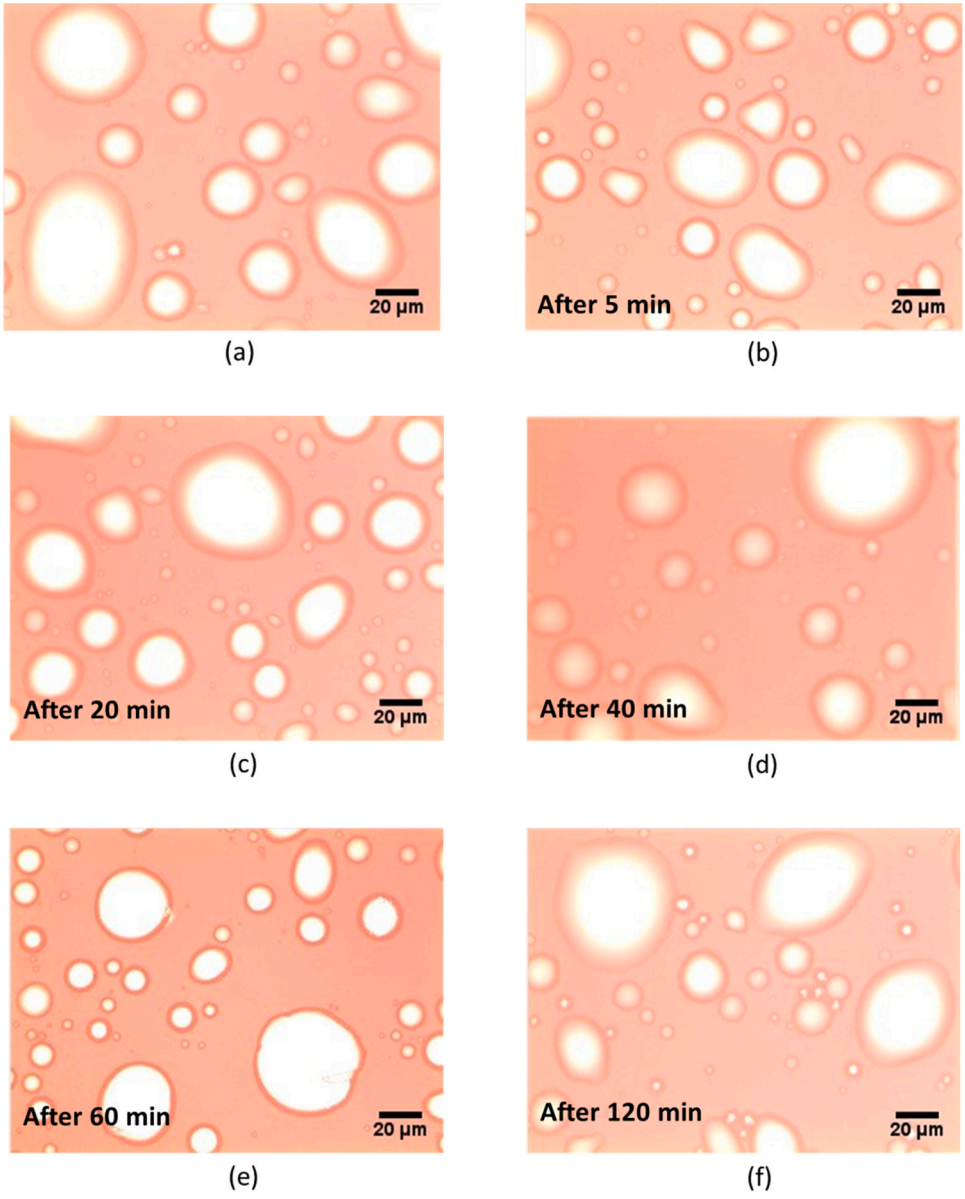

Fig. 5. Microscopic view of emulsion sample under static conditions (a) immediately after preparation, (b) 5 min after preparation, (c) 20 min after preparation, (d) 40 min after preparation, (e) 60 min after preparation, and (f) 120 min after preparation.

The emulsion had different sizes of water droplets at 0 min of sampling (Fig. 5), with some as large as 200 μm (Fig. 6). When injected into the micromodel under these conditions, the emulsion can create pore blockages, allowing the study of ultrasonic application to be conducted. The droplets appeared to be stabilized over the two hours of sampling, as depicted in Figs. 5 and 6. At 120 min of sampling, some large droplets had broken down into smaller droplets, resulting in an increase in stable smaller droplets with sizes of 20 μm occurring the most. As the size of the emulsion droplets decreases, emulsion stability increases [26]. Although stable emulsions can be beneficial for enhanced oil recovery, in some circumstances (especially in heavy oil reservoirs), they can pose problems and cause formation damage, as is the case in this study. The emulsion can clog the micromodel pores, impede or redirect oil flow, or increase the viscosity of the oil, causing loss of pressure and production decline. Therefore, the synthetized emulsions was found to be appropriate for the micromodel flooding based on the above analysis.

3.2. Mechanism for emulsion plugging in micromodel pores and throats

An understanding of how the flow of the preprared emulsion could plug the micromodel's pores and throats and impede recovery performance is provided by a pore-scale examination of the flow of emulsion in the micromodel. Fig. 7 depicts the processes that resulted in emulsion plugging in the micromodel's pores and throats. The water droplets and oil phase are represented by the white and brown areas, respectively.

The behavior of emulsion under dynamic conditions was distinct from those under static conditions (Figs. 5 and 7). Under dynamic conditions, it can be seen that some of the emulsion droplets aggregated and completely plugged the micromodel's pore throat (Fig. 7a). Larger droplets were also formed which can be explained by droplet coalescence when the interfacial films in some aggregated droplets break (Fig. 7b). The large droplets have the potential to obstruct a sizable portion of the pore body or throat. The pore throat area that is open to emulsion flow was also limited by other droplets adhering to the pore body and throat surfaces (Fig. 7c) through an intercepting process. All the described actions limit the pore network of the micromodel, thus diverting the flow of fluids in the affected area.

3.3. Pore scale analysis of the micromodel pores and throats under ultrasonic waves

To analyze the behavior of the emulsion during water flooding and under the influence of ultrasonic waves, pore scale analysis was carried out in micromodel pores distant from the waterfront. Fig. 8 illustrates the elimination process of droplet aggregation, at the pore scale, by ultrasonic waves (20 kHz, 100 Watt) at different sonication times, and their corresponding frequency distributions of droplet sizes.

Before the application of ultrasound, it could be seen that various droplet sizes aggregated to create a complete blockage at the left side of the pore-throat region (Fig. 8a). Droplet aggregation happens because of Brownian forces and when the repulsive energy is less than the van der Waals energy [27]. The van der Waals attraction grows as the distance between the droplets decreases, and at short separation distances, the attraction becomes extremely strong, causing droplet aggregation [28]. This behavior is undesirable because it promotes pore blockages by bringing droplets closer together. The flow of fluid appeared to have not affected the pore-throat blockages two hours before the introduction of ultrasound. However, the introduction of ultrasound resulted in droplet coalescence and the rupturing of some of the droplets at 40 min of sonication (Fig. 8b), followed by gradual removal of the pore throat blockages at 80 min of sonication, which is caused by droplet coalescence and disbandment of aggregated droplets as shown on the image and droplet size frequency distribution plot (Fig. 8c). Droplet coalescence, droplet buoyancy or sedimentation, and finally, droplet rupturing are three steps of demulsification process. Dispersed phase droplets first go to high-pressure zones, where they progressively clump together. As

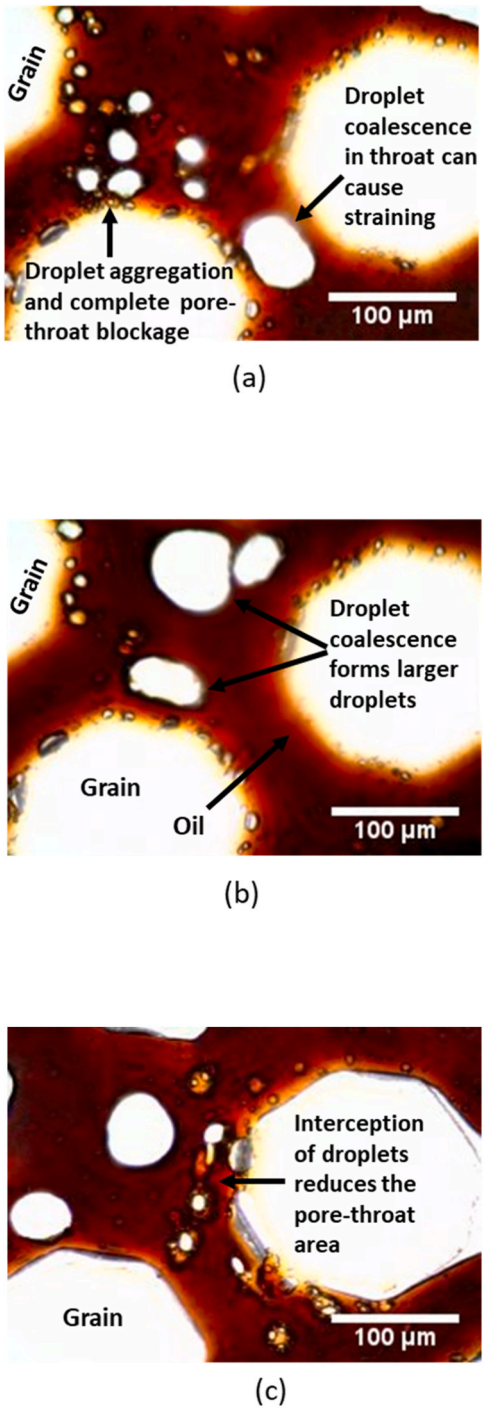

Fig. 7. Microscopic view of the flow of emulsion in different regions of the micromodel at the pore level under dynamic conditions (a) pore throat complete plugging (b) droplet coalescence, and (c) interception of water droplets. Flow direction is from left to right.

the droplets approach one another, the interface film prevents the droplets from coalescing. Hence, the interface film must be ruptured to ensure effective coalescence and droplet breakdown. The aggregated droplets and the film is ruptured if the ultrasonic strength exceeds the energy barrier and short-range repulsion forces [29–31]. As a result, the droplets combine to create a single bigger droplet (Fig. 8b) that rises to the surface owing to buoyancy force, causing the emulsion droplet to break. As a result, it was found that the key to ultrasonic demulsification is the droplets' coalescence. The image and frequency distribution of

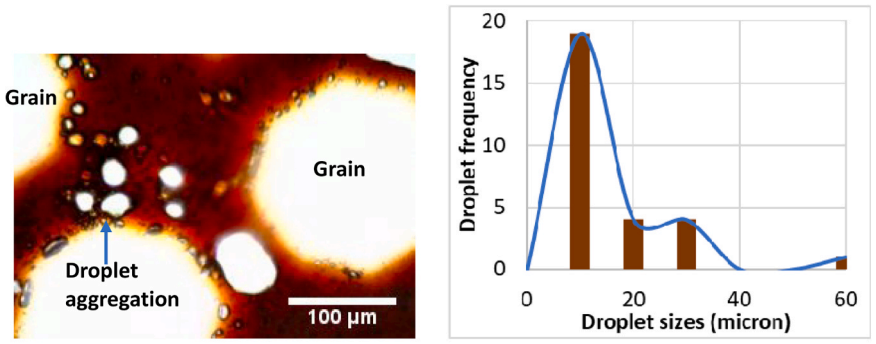

(a)

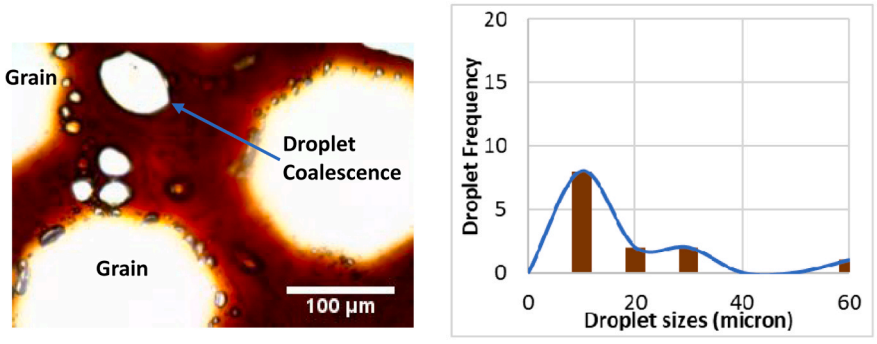

(b)

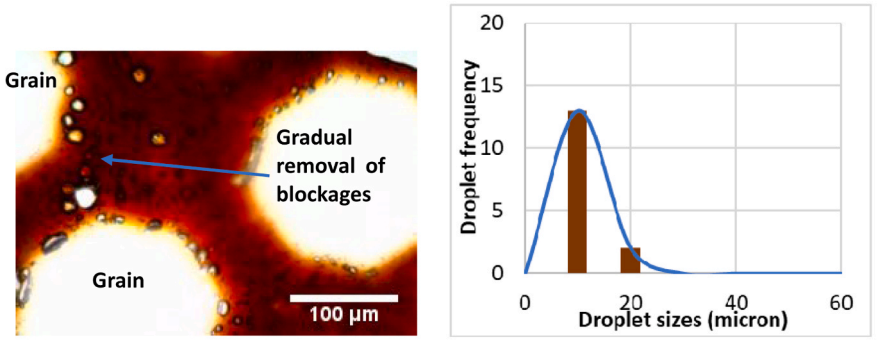

(c)

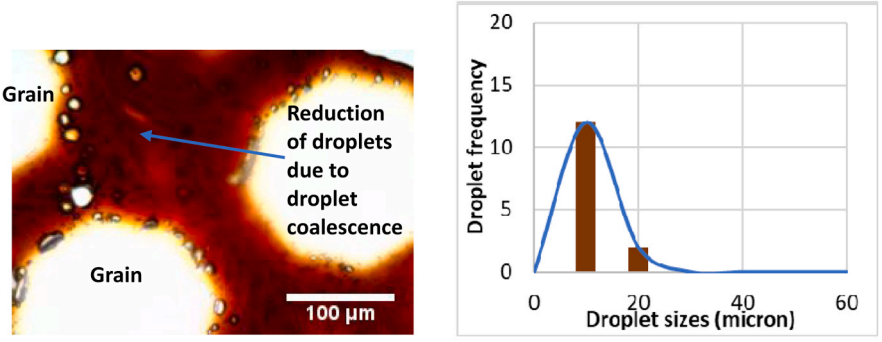

(d)

Fig. 8. Droplet aggregation removal under dynamic conditions, at pore scale, by ultrasonic waves (20 kHz, 100 Watt) at different sonication times, and their corresponding frequency distributions of droplet sizes in the circle patterned micromodel (a) 0 min (b) 40 min (c) 80 min, and (d) 120 min. Flow direction is from left to right.

droplet sizes in Fig. 8d demonstrate a considerable reduction in the number of emulsion droplets at 120 min of sonication as compared to the emulsion droplets before ultrasound (Fig. 8a), which is attributable to the coalescing process induced by ultrasound. After 2 h of sonication, ultrasound at low power (100 watt) and low frequency (20 kHz) partially removed the blockages while also establishing a flow path at the pore throat.

Fig. 9 shows the elimination process of droplet interception, at pore scale, by ultrasonic waves (20 kHz, 100 Watt) at different sonication times, and their corresponding frequency distributions of droplet sizes.

It was evident from the comparison of the images and frequency distribution of droplet sizes (Fig. 9a-d), that the use of ultrasound promoted the breakdown of emulsion droplets. There was a blockage in the area where droplets had adsorbed on the right side of the pore throat surface, which could restrict the flow of fluid (Fig. 9a). Surface forces are primarily responsible for this capture of droplets by interception, and if droplet interception results in a reduction in diameter, it may prompt additional droplets to start straining, which will result in more blockages [32]. Breakdown of both big and small droplets was observed after 40 min of sonication (Fig. 9b), followed by movement of the droplets and progressive elimination of droplet interception at 80 min of sonication (Fig. 9c). Finally, the droplet plugs at the pore throat were removed, and the droplets were dispersed in the pore (Fig. 9d). A comparison of the frequency distribution of droplet sizes in Figs. 9a and 9d reveals that the larger droplets (50–60 μm) have all ruptured due to coalescence, and the number of smaller droplets (up to 20 μm) has been reduced by ultrasonic demulsification.

When applied at higher power, Fig. 10 demonstrates the pore scale evidence of ultrasound's potential to cause emulsification. The observed emulsification at pore scale, by ultrasonic waves (20 kHz, 1000 Watt) at different sonication times, and their corresponding frequency distributions of droplet sizes are presented.

At the same frequency of 20 kHz, the use of high ultrasonic power of 1000 watt resulted in emulsification, as shown in Fig. 10 (a-d). When high ultrasonic power is applied, the agitation transmitted to the micromodel rises because of increased mechanical vibrations, and if emulsion is agitated excessively after it has broken down, re-emulsification can occur [33]. The frequency distribution of the droplet sizes revealed that the droplets increased by nearly 50 % after 2 h of sonication (Fig. 10a and d). Emulsification is undesirable because the breakdown processes may induce pore throat blockages and limit oil mobility. Therefore, the employment of high power (1000 watt) was found to have a negative effect on ultrasonic demulsification.

The mechanism for ultrasound-induced demulsification at low power (100 watt) and low frequency (20 kHz) was observed to be droplet coalescence induced by vibrations. Ultrasound creates mechanical vibrations in the micromodel, which causes droplets of various sizes to vibrate at different speeds and collide with one another, allowing the droplets to coalesce and the interfacial film to rupture. In addition, the heat produced by ultrasound can also reduce the viscosity of emulsions and the strength of interfacial films, lowering the hydrodynamic drag force and allowing water drops to collide and coalesce [3,5,34].

3.4. *Effects of ultrasound properties on the removal of emulsion plugging across the whole micromodel*

The flow of emulsion in the micromodel was exposed to ultrasonic waves at different ultrasonic powers, frequencies, and treatment times, and how a change in these ultrasonic parameters affects recovery was examined. To achieve a standard deviation, each experiment was performed three times, and the data was also provided with an error bar. The error bars in the charts at each point represent the measurement findings' difference from their average.

Fig. 11 shows the influence of varying ultrasonic power on recovered emulsions during sonication of the micromodel.

Fig. 11 indicates that increasing the ultrasound power from 100 watt to 1000 watt significantly affects the demulsification process. The recovered emulsions are much lower for the higher ultrasound power throughout the sonication period. This could be due to several factors, including the potential for higher ultrasound power to cause emulsification and enhanced blockages in the micromodel, thereby reducing their recoverability. It is important to note that other factors such as the nature and composition of the emulsions could play a role in these results. Generally, the rate of recovery of emulsions appears to be faster for the lower ultrasound power. This is evident by comparing the percentage increase in recovered emulsions from 20 to 120 min, 11 % increase for 100 watts compared to 10.3 % increase for 1000 watt, indicating that the demulsification process is more efficient at lower ultrasound power of 100 watt.

As the sonication period progresses, the percentage of recovered emulsions increases at ultrasound power of 100 watt. Although, longer exposure to ultrasound at 100 watt contributes to the demulsification process in the micromodel and improved emulsion recovery, the effect of ultrasound on the recovered emulsions seems to diminish over time. For example, the increase from 57 % to 58 % over 60–120 min is smaller compared to the increase from 46.9 % to 57 % over 20–60 min for the 100-watt power. This could imply that after a certain point, additional exposure to ultrasound might not have a significant impact on the emulsions. This result was consistent with the pore scale investigations where ultrasound at 100 watts removed the droplet plug which in turn improved fluid mobility. Although the application of ultrasound at 100 watt was advantageous to emulsion recovery, Fig. 11 shows that by increasing the applied ultrasonic power from 100 to 1000 watts, the percentage of recovered emulsions from the micromodel is decreased. As the applied power of ultrasound is increased, the degree of vibration it produces improves, causing more agitation of emulsions and re-emulsification [33].

Furthermore, cavitation is produced when the ultrasonic intensity exceeds the energy associated with the attraction interactions between the liquid molecules, resulting in the formation of cavitation bubbles. The shock waves and high-speed micro jets created by the bubble collapse can obstruct droplet migration and disrupt droplet bandings, resulting in low demulsification efficiency [14]. Secondary emulsification is also caused by ultrasonic cavitation, which disperses microscopic oil droplets into separated water [3,5]. These processes explain the negative effect of increasing ultrasonic power during ultrasonic demulsification. Compared to the case of no ultrasound, it could be seen that ultrasonic treatment became worse for higher than 100-watt power input (Fig. 11). This analysis indicates that at a constant frequency of 20 kHz, excessive ultrasonic power is undesirable for the treatment of emulsion plugging in the reservoir. Amongst the range of ultrasonic powers considered in this study, only the power output of 100 watt was found to be suitable for promoting demulsification and recovery of additional emulsions from the micromodel.

Fig. 12 shows how a change in ultrasonic frequency affects emulsion recovery from the micromodel at a constant optimum power of 100 watt.

It can be observed that the proportion of recovered emulsions is somewhat greater at 20 kHz than at 40 kHz, meaning that the 20 kHz's water droplet coalescence effect is superior to the 40 kHz's. A lower frequency correlates to a longer wavelength, resulting in a faster rate of coalescence for a given pair of droplets [4]. Another explanation may be found in the equation for the amplitude of the acoustic wave in water-in-oil emulsions [35]:

$$A = \frac{\sqrt{(Ic_o)}}{\sqrt{(2\pi f \rho_o)}}$$

Where A is the amplitude of the acoustic wave in water-in-oil emulsions, f is the frequency and ρ_o is the oil density. According to the equation, as the frequency decreases, the amplitude of the acoustic wave increases. The continuous phase oscillation of droplets is facilitated by increasing

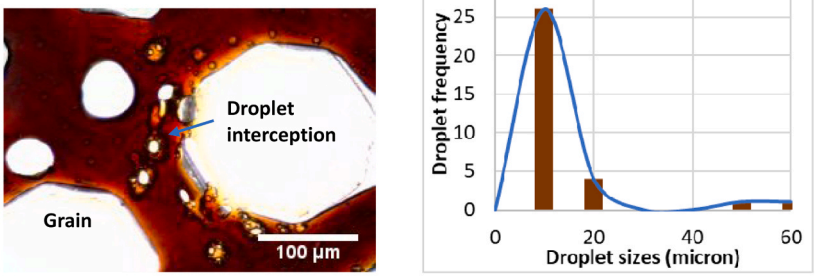

(a)

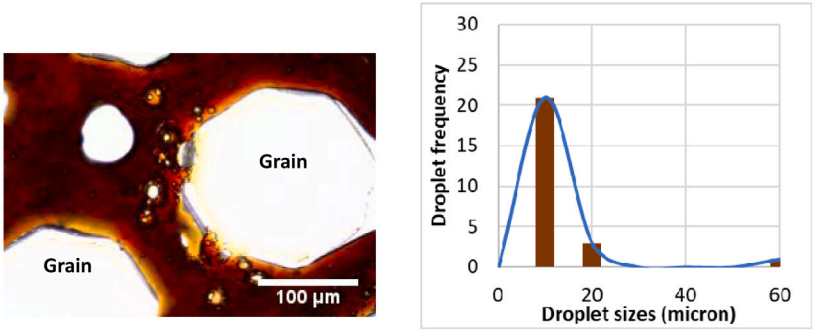

(b)

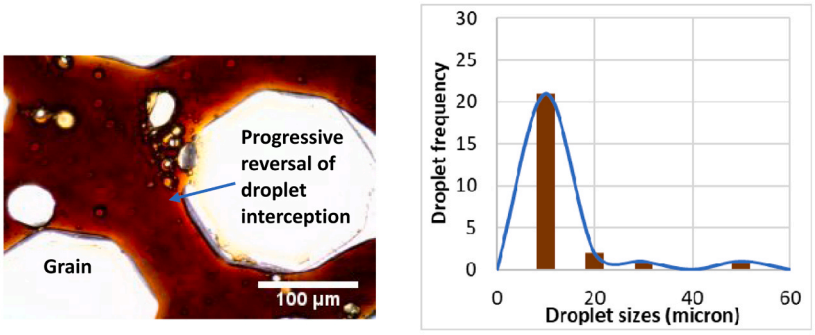

(c)

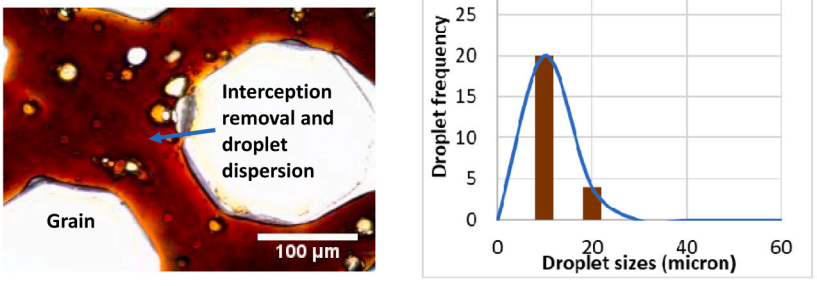

(d)

Fig. 9. Droplet interception removal under dynamic conditions, at pore scale, by ultrasonic waves (20 kHz, 100 Watt) at different sonication times, and their corresponding frequency distributions of droplet sizes in the circle patterned micromodel (a) 0 min (b) 40 min (c) 80 min, and (d) 120 min. Flow direction is from left to right.

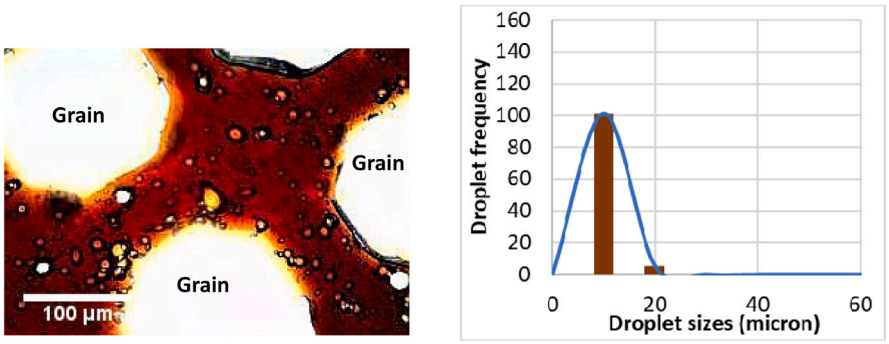

(a)

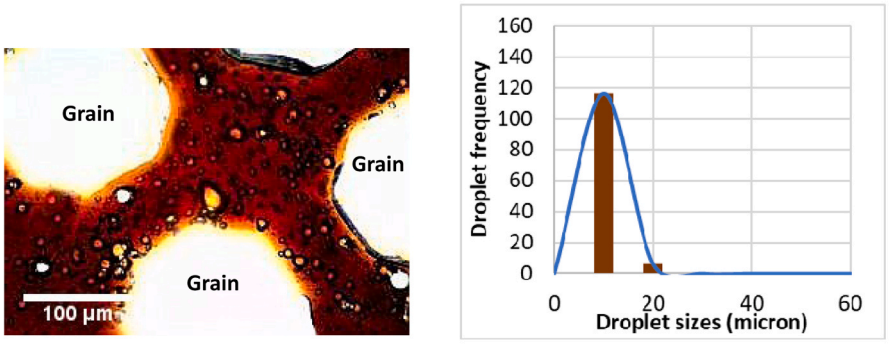

(b)

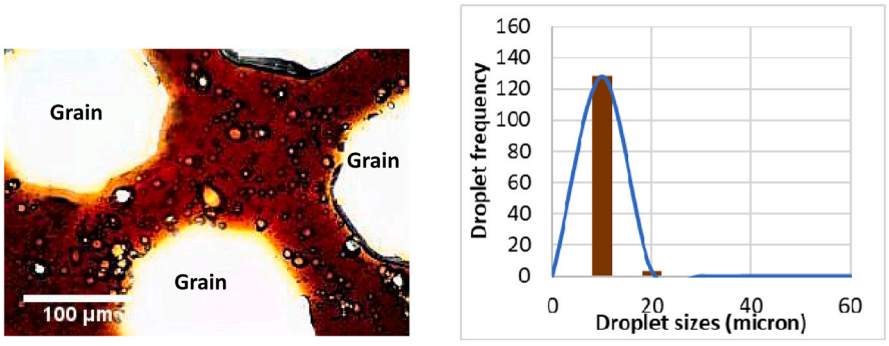

(c)

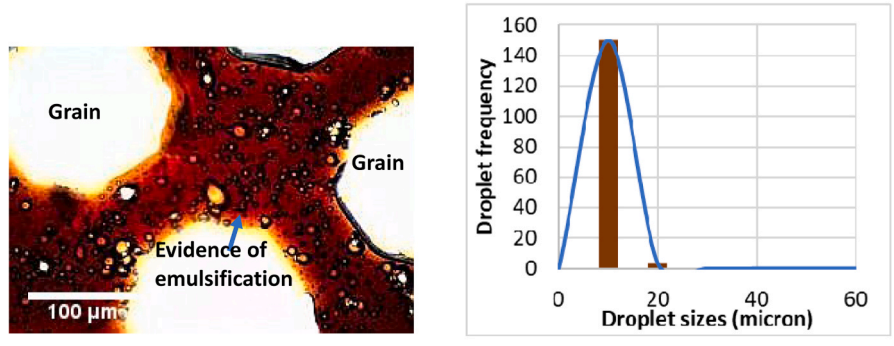

(d)

Fig. 10. Emulsification at pore scale under dynamic conditions, by ultrasonic waves (20 kHz, 1000 watt) at different sonication times, and their corresponding frequency distributions of droplet sizes in the circle patterned micromodel (a) 0 min (b) 40 min (c) 80 min, and (d) 120 min. Flow direction is from left to right.

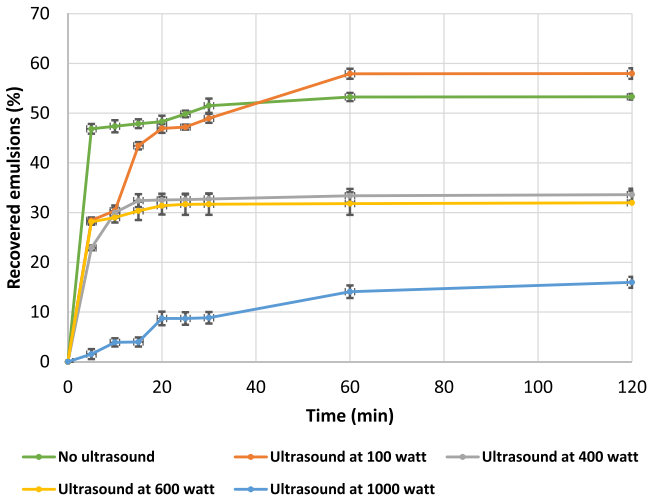

Fig. 11. Influence of varying ultrasonic power on recovered emulsions during sonication of the micromodel at a constant frequency of 20 kHz.

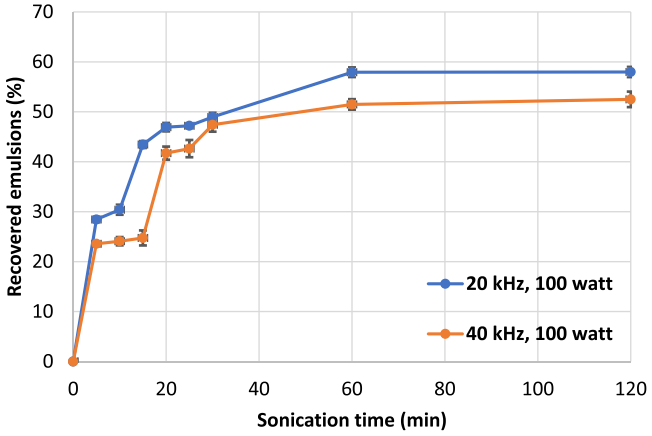

Fig. 12. Effect of a change in ultrasonic frequency on recovered emulsions during sonication of the micromodel at a constant power of 100 watt.

the acoustic wave amplitude, which prevents the droplets from migrating towards the pressure node and improves their coalescence. The principal acoustic force causes dispersed droplets to come together and form bandings when the frequency is increased. The interfacial film, on the other hand, cannot be broken and obstructs droplet coalescence, resulting in reduced demulsification efficiency [35].

In terms of the effect of a change in the ultrasonic treatment time, the emulsion droplets are predicted to coalesce when the treatment time is extended owing to acoustic pressures. The coalesced droplets would then be grown until they reached a critical size, at which point they would rupture. The visualization of the whole micromodel before and after ultrasonic treatment at 20 kHz and 100 watts is shown in Fig. 13. The images have been segmented for colour distinction of the phases, using three-phase Trainable Weka Segmentation, a plugin in ImageJ.

The demulsification effectiveness of ultrasound treatment improves as treatment time increases, and as a consequence, more emulsions are recovered from the micromodel. Fig. 13 shows how the ultrasound treatment effect stabilizes after 60 min. After 60 min of treatment, increasing the treatment duration does not contribute to the percentage of recovered emulsions. Due to the huge number of nuclei in emulsion, excessive treatment duration could induce significant acoustic cavitation just like in the case of ultrasonic power. This causes previously coalesced droplets to disperse, lowering demulsification effectiveness. Additionally, more effect of cavitation might hinder ultrasound's impact on emulsions by lowering the efficiency of ultrasound's energy [36]. As a result, for efficient demulsification, the treatment duration should be adjusted to an ideal value. In this test, 60 min was shown to be the best treatment time at 20 kHz to save cost and time. It is notable that the removal of emulsion plugging depends on the intensity of the acoustic field surrounding the glass micromodel. The acoustic intensity can be reduced when the 5 cm distance between the ultrasonic transducers and micromodel increases [37]. Therefore, it is recommended for future studies to clarify the effect of the distance between the ultrasonic transducers and micromodel on emulsion plugging. Additionally, combining ultrasound with conventional techniques may improve the removal efficiency of emulsion plugging [38]. The use of dual-frequency ultrasound and cutting-edge ultrasound equipment may also increase the effectiveness of removal [39,40].

At the field level, ultrasonic transducers positioned opposite the bottom-hole production intervals, can emit ultrasonic waves into the reservoir and eliminate near-wellbore damage caused by emulsion plugging, thus enhancing oil flow into the wellbore [38]. Hence, the findings of this study give insights into the impact of different ultrasonic properties (power, frequency) on the demulsification process, as well as the behavior of the emulsions themselves, allowing petroleum engineers to optimize ultrasound demulsification strategies.

4. Important macroscopic properties to consider

Temperature is an important macroscopic property influenced by the action of ultrasound. The heat generated by ultrasound increases the temperature of the system and reduces viscosity. Higher viscosity oil can hold up more and larger water droplets than lower viscosity oil [39]. The heat action of ultrasound reduces the viscosity of emulsions and the strength of interfacial films, lowering the hydrodynamic drag force and allowing water droplets to collide and coalesce [3,5,34]. The viscosity of emulsions reduces with increasing temperature, thus increasing the frequency of droplet collisions [40]. For higher optimal ultrasonic power, this impact will be more pronounced. According to research, to demulsify the emulsions when the oil viscosity is high, a higher optimal ultrasonic power is needed [6]. However, experiments in this study have revealed that excessive ultrasonic power (400–1000 watt) would hinder ultrasound demulsification. Moreover, excessive heat can cause the loss of light fractions of crude.

Figs. 14 and 15 provide further evidence of ultrasound-induced heat production. Figs. 14 and 15 shows the effect of ultrasound on the water temperature in the bath during experiments at constant frequencies, different powers, and a maximum sonication time of 120 min. The temperature of the water bath rises with an increase in ultrasonic power and sonication time, with a maximum increase observed at 1000 watt and 120 min sonication, for both frequencies 20 and 40 kHz. This heating action could increase the temperature of the micromodel system that is in direct contact with the water. However, this study did not consider how long it takes for heat to transfer into the micromodel system.

Another factor to consider is the strength of the reservoir. Under the influence of ultrasound, clay detachment and particle migration are more likely to occur in unconsolidated sandstone reservoirs, and this possibility grows as the ultrasonic power increases [41]. However, this scenario is not expected in a glass micromodel system or a consolidated reservoir.

5. Conclusions

The effect of ultrasonic waves on the removal of emulsion plugging in an oil reservoir was studied using a two-D glass micromodel. Microscopic evidence showed that ultrasonic stimulation at low power of 100 watt is an effective technique to facilitate droplet coalescence, being the main mechanism to break down stable water-in-oil emulsions and remediate pore plugging. As the ultrasonic power is increased to

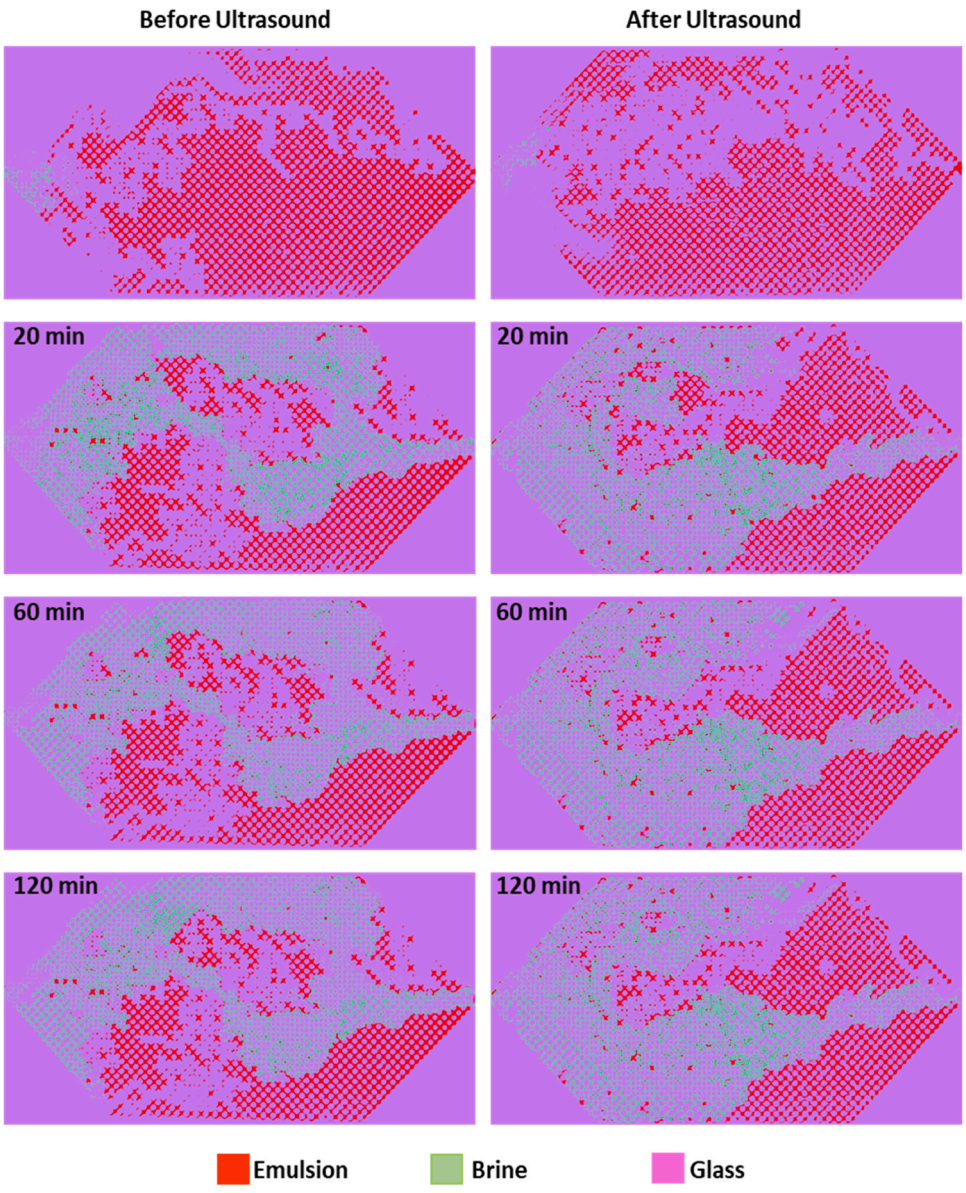

Fig. 13. Visualization of the whole micromodel before and after ultrasound application at 20 kHz and 100 watts. Flow direction is from left to right.

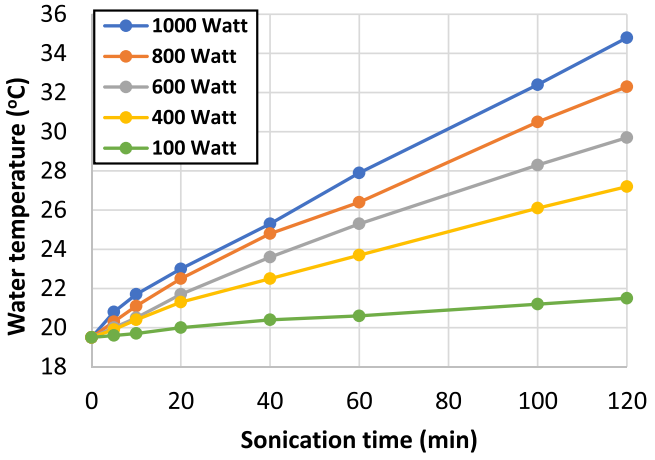

Fig. 14. Effect of ultrasound on the temperature of water in bath at constant ultrasonic frequency 20 kHz and different powers (watt).

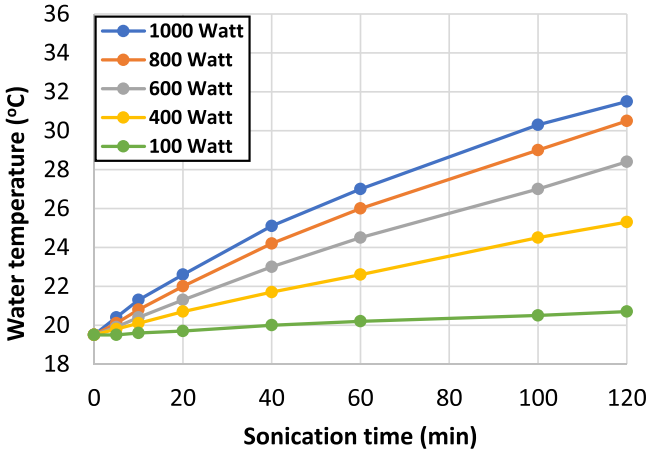

Fig. 15. Effect of ultrasound on the temperature of water in bath at constant ultrasonic frequency 40 kHz and different powers (watt).

1000 W, the possibility of cavitation sets in, resulting in secondary emulsification and a reduction in demulsification efficiency. Similarly, the increase of ultrasonic frequency from 20 to 40 kHz, causes demulsification effectiveness to decrease and less emulsion recovered from the micromodel. Another mechanism attributed to ultrasound demulsification is the heat produced by ultrasound which increases the system's temperature while lowering the emulsion's viscosity. As the viscosity and interfacial tension of the emulsions reduce, the risk of emulsion plugging in the reservoir lowers.

In the petroleum industry, emulsion plugging-related near-wellbore damage can be removed by using ultrasonic transducers positioned opposite bottom-hole production intervals to send ultrasonic waves into the reservoir. The results of this study thus enable petroleum engineers to optimize ultrasound demulsification methods by providing insights into the effects of various ultrasonic properties (power, frequency) on the demulsification process as well as the behavior of the emulsions themselves.

Ethics approval

Not applicable.

Consent to participate

Not applicable.

Consent for publication

Not applicable.

Code availability

Not applicable.

Funding

This work was funded by Tertiary Education Trust Fund – TETFund of Nigeria (grant number RG14381-10) through the award of a PhD scholarship to Ephraim Otumudia.

CRediT authorship contribution statement

Ephraim Otumudia: Conceptualization, Methodology, Validation, Formal analysis, Investigation, Resources, Data curation, Writing – original draft, Writing – review & editing, Visualization, Project administration, Funding acquisition. **Hossein Hamidi:** Conceptualization, Methodology, Validation, Resources, Writing – review & editing, Project administration, Supervision, Funding acquisition. **Prashant Jadhawar:** Conceptualization, Supervision, Writing – review & editing. **Kejian Wu:** Conceptualization, Supervision, Writing – review & editing.

Declaration of Competing Interest

The authors declare that they have no known competing financial interests or personal relationships that could have appeared to influence the work reported in this paper.

Data availability

Data will be made available on request.

Acknowledgement

The authors are grateful to the Tertiary Education Trust Fund (TETFund) of Nigeria and University of Aberdeen UK, for providing the laboratory facilities required to complete this research.

References

[1] L. Yu, M. Han, F. He, A review of treating oily wastewater, Arab. J. Chem. 10 (2017) S1913–S1922, https://doi.org/10.1016/j.arabjc.2013.07.020.
[2] Z. Grenoble, S. Trabelsi, Mechanisms, performance optimization and new developments in demulsification processes for oil and gas applications, Adv. Colloid Interface Sci. 260 (2018) 32–45, https://doi.org/10.1016/j.cis.2018.08.003.
[3] X. Luo, H. Gong, J. Cao, H. Yin, Y. Yan, L. He, Enhanced separation of water-in-oil emulsions using ultrasonic standing waves, Chem. Eng. Sci. 203 (2019) 285–292, https://doi.org/10.1016/j.ces.2019.04.002.
[4] B. Pal, R. Kumar, T.K. Naiya, Demulsification of crude oil-water emulsion using naturally formulated demulsifier, Pet. Sci. Technol. 39 (2021) 1027–1042, https://doi.org/10.1080/10916466.2021.1983599.
[5] W. Xie, R. Li, X. Lu, P. Han, S. Gu, Acoustically aided coalescence of water droplets and dehydration of crude oil emulsion, Korean J. Chem. Eng. 32 (2015) 643–649, https://doi.org/10.1007/s11814-014-0253-6.
[6] X. Luo, J. Cao, H. Gong, H. Yan, L. He, Phase separation technology based on ultrasonic standing waves: a review, Ultrason Sonochem. 48 (2018) 287–298, https://doi.org/10.1016/j.ultsonch.2018.06.006.
[7] F.G. Antes, L.O. Diehl, J.S.F. Pereira, et al., Feasibility of low frequency ultrasound for water removal from crude oil emulsions, Ultrason. Sonochem. 25 (2015) 70–75, https://doi.org/10.1016/j.ultsonch.2015.01.003.
[8] A. Khajehesamedini, A. Sadatshojaie, P. Parvasi, M. Reza Rahimpour, M. Mehdi Naserimojarad, Experimental and theoretical study of crude oil pretreatment using low-frequency ultrasonic waves, Ultrason Sonochem. 48 (2018) 383–395, https://doi.org/10.1016/j.ultsonch.2018.05.032.
[9] M. Mohsin, M. Meribout, Oil–water de-emulsification using ultrasonic technology, Ultrason. Sonochem. 22 (2015) 573–579, https://doi.org/10.1016/j.ultsonch.2014.05.014.
[10] C.M.G. Atehortúa, N. Pérez, M.A.B. Andrade, L.O.V. Pereira, J.C. Adamowski, Water-in-oil emulsions separation using an ultrasonic standing wave coalescence chamber, Ultrason Sonochem. 57 (2019) 57–61, https://doi.org/10.1016/j.ultsonch.2019.04.043.
[11] S. Nii, S. Kikumoto, H. Tokuyama, Quantitative approach to ultrasonic emulsion separation, Ultrason Sonochem. 16 (2009) 145–149, https://doi.org/10.1016/j.ultsonch.2008.07.005.
[12] Garcia-Lopez A., Sinha D., Enhanced Acoustic Separation of Oil-Water Emulsion in Resonant Cavities. 2008.
[13] J. Jiao, Y. He, T. Leong, et al., Experimental and theoretical studies on the movements of two bubbles in an acoustic standing wave field, J. Phys. Chem. B 117 (2013) 12549–12555, https://doi.org/10.1021/jp404886h.
[14] G.R. Check, D. Mowla, Theoretical and experimental investigation of desalting and dehydration of crude oil by assistance of ultrasonic irradiation, Ultrason Sonochem. 20 (2013) 378–385, https://doi.org/10.1016/j.ultsonch.2012.06.007.
[15] A. Mehranfar, M.H. Ghazanfari, Investigation of the microscopic displacement mechanisms and macroscopic behavior of alkaline flooding at different wettability conditions in shaly glass micromodels, J. Pet. Sci. Eng. 122 (2014) 595–615, https://doi.org/10.1016/j.petrol.2014.08.027.
[16] H. Doryani, M.R. Malayeri, M. Riazi, Visualization of asphaltene precipitation and deposition in a uniformly patterned glass micromodel, Fuel 182 (2016) 613–622, https://doi.org/10.1016/j.fuel.2016.06.004.
[17] S. Maaref, S. Ayatollahi, N. Rezaei, M. Masihi, The effect of dispersed phase salinity on water-in-oil emulsion flow performance: a micromodel study, Ind. Eng. Chem. Res. 56 (2017) 4549–4561, https://doi.org/10.1021/acs.iecr.7b00432.
[18] M. Sharifipour, P. Pourafshary, A. Nakhaee, Study of the effect of clay swelling on the oil recovery factor in porous media using a glass micromodel, Appl. Clay Sci. 141 (2017) 125–131, https://doi.org/10.1016/j.clay.2017.02.020.
[19] W.- Bartels, H. Mahani, S. Berg, R. Menezes, dH. van, A. Fadili, Low salinity flooding (LSF) in sandstones at pore scale: micro-model development and investigation, SPE Annu. Tech. Conf. Exhib. (2016), https://doi.org/10.2118/181386-MS.
[20] B. Yadali Jamaloei, K. Asghari, R. Kharrat, F. Ahmadloo, Pore-scale two-phase filtration in imbibition process through porous media at high- and low-interfacial tension flow conditions, J. Pet. Sci. Eng. 72 (2010) 251–269, https://doi.org/10.1016/j.petrol.2010.03.026.
[21] B. Yadali Jamaloei, R. Kharrat, Pore-scale description of surfactant-enhanced waterflooding for heavy oil recovery, J. Pet. Sci. Eng. 92–93 (2012) 89–101, https://doi.org/10.1016/j.petrol.2012.06.001.
[22] Sepideh Maaref, Shahab Ayatollahi, The effect of brine salinity on water-in-oil emulsion stability through droplet size distribution analysis: a case study, J. Dispers. Sci. Technol. 39 (5) (2018) 721–733, https://doi.org/10.1080/01932691.2017.1386569.
[23] W. Liu, D. Sun, C. Li, Q. Liu, J. Xu, Formation and stability of paraffin oil-in-water nano-emulsions prepared by the emulsion inversion point method, J. Colloid Interface Sci. 303 (2006) 557–563, https://doi.org/10.1016/j.jcis.2006.07.055.
[24] M. Arhuoma, M. Dong, D. Yang, R. Idem, Determination of water-in-oil emulsion viscosity in porous media, Ind. Eng. Chem. Res. 48 (2009) 7092–7102, https://doi.org/10.1021/ie801818n.
[25] N. Rezaei, A. Firoozabadi, Macro- and microscale waterflooding performances of crudes which form w/o emulsions upon mixing with brines, Energy Fuels 28 (2014) 2092–2103, https://doi.org/10.1021/ef402223d.
[26] M. Moradi, V. Alvarado, S. Huzurbazar, Effect of salinity on water-in-crude oil emulsion: evaluation through drop-size distribution proxy, Energy Fuels 25 (2011) 260–268, https://doi.org/10.1021/ef101236h.

[27] L. Payet, E.M. Terentjev, Emulsification and stabilization mechanisms of O/W emulsions in the presence of chitosan, Langmuir 24 (2008) 12247–12252, https://doi.org/10.1021/la8019217.
[28] T.F. Tadros, Emulsion Formation and Stability, John Wiley & Sons, Incorporated, Weinheim, 2013.
[29] G.D. Pangu, D.L. Feke, Acoustically aided separation of oil droplets from aqueous emulsions, Chem. Eng. Sci. 59 (2004) 3183–3193, https://doi.org/10.1016/j.ces.2004.03.038.
[30] G. Ye, X. Lu, P. Han, F. Peng, Y. Wang, X. Shen, Application of ultrasound on crude oil pretreatment, Chem. Eng. Process. Process Intensif. 47 (2008) 2346–2350, https://doi.org/10.1016/j.cep.2008.01.010.
[31] H.G. Nasiri, R. Kadkhodaee, M.T. Hamed Mousavian, Flocculation and separation of oil droplets in ultrasonic standing wave field, Sep. Sci. Technol. 47 (2012) 1985–1990, https://doi.org/10.1080/01496395.2012.661824.
[32] I. Azizov, M. Dudek, G. Øye, Emulsions in porous media from the perspective of produced water re-injection – a review, J. Pet. Sci. Eng. 206 (2021), 109057, https://doi.org/10.1016/j.petrol.2021.109057.
[33] G. Leopold, Breaking produced-fluid and process-stream emulsions. in: Anonymous Emulsions, American Chemical Society, 1992, pp. 341–383.
[34] F.J. Trujillo, P. Juliano, G. Barbosa-Cánovas, K. Knoerzer, Separation of suspensions and emulsions via ultrasonic standing waves – a review, Ultrason. Sonochem. 21 (2014) 2151–2164, https://doi.org/10.1016/j.ultsonch.2014.02.016.
[35] X. Luo, H. Gong, H. Yin, Z. He, L. He, Optimization of acoustic parameters for ultrasonic separation of emulsions with different physical properties, Ultrason. Sonochem. 68 (2020), 105221, https://doi.org/10.1016/j.ultsonch.2020.105221.
[36] I. Adeyemi, M. Meribout, L. Khezzar, Recent developments, challenges, and prospects of ultrasound-assisted oil technologies, Ultrason. Sonochem. 82 (2022), 105902, https://doi.org/10.1016/j.ultsonch.2021.105902.
[37] G.J. Price, N.K. Harris, A.J. Stewart, Direct observation of cavitation fields at 23 and 515kHz, Ultrason. Sonochem. 17 (1) (2010) 30–33, https://doi.org/10.1016/j.ultsonch.2009.04.009.
[38] H. Hamidi, A. Sharifi Haddad, E.W. Otumudia, R. Rafati, E. Mohammadian, A. Azdarpour, W. Giles Pilcher, P. Wilhelm Fuehrmann, L. Ricardo Sosa, N. Cota, D. Cruz García, R.M. Ibrahim, M. Damiev, E. Tanujaya, Recent applications of ultrasonic waves in improved oil recovery: a review of techniques and results, Ultrasonics (2021) 110.
[39] A.M. Al-Sabagh, N.M. Nasser, T.M. Abd El-Hamid, Investigation of kinetic and rheological properties for the demulsification process, Egypt. J. Pet. 22 (2013) 117–127, https://doi.org/10.1016/j.ejpe.2012.11.013.
[40] Kokal S., Wingrove M., Emulsion Separation Index: From Laboratory to Field Case Studies. SPE Annual Technical Conference and Exhibition, 2000. ⟨doi:10.2118/63165-MS⟩.
[41] E. Otumudia, H. Hamidi, P. Jadhawar, K. Wu, The utilization of ultrasound for improving oil recovery and formation damage remediation in petroleum reservoirs: review of most recent researches, Energies (2022) 15, https://doi.org/10.3390/en15134906.